JOURNAL OF PHYSICAL ORGANIC CHEMISTRY
J. Phys. Org. Chem. 2002; **15:** 270–277
Published online in Wiley InterScience (www.interscience.wiley.com). DOI: 10.1002/poc.479

The role of specific interactions in crystalline complex formation. Structural and thermochemical analysis of inclusion compounds of *cis*- and *trans*-9,10-bis(4-bromophenyl)-9,10-dihydroxy-9,10-dihydroanthracene with dimethyl sulfoxide

Thomas H. Brehmer,[1] Ralf Kirchner,[2] Jürgen Seidel[2]* and Edwin Weber[1]*

[1]Institut für Organische Chemie, TU Bergakademie Freiberg, Leipziger Strasse 29, D-09596 Freiberg/Sachsen, Germany
[2]Institut für Physikalische Chemie, TU Bergakademie Freiberg, Leipziger Strasse 29, D-09596 Freiberg/Sachsen, Germany

Received 19 September 2001; revised 20 December 2001; accepted 15 January 2002

epoc

ABSTRACT: Referring to a crucial problem in crystal engineering and co-crystallization of host–guest complexes, whether the non-covalent supramolecular interactions existing in a pre-crystalline solution state may determine the subsequent crystal structure, the particular inclusion properties of host compounds **1**, *cis*- and **2**, *trans*-9,10-bis(4-bromophenyl)-9,10-dihydroxy-9,10-dihydroanthracene, with dimethyl sulfoxide (DMSO) were studied by using x-ray structure analysis and calorimetric methods. Both hosts form crystalline inclusion complexes with DMSO showing 2:3 (**1**·DMSO) and 1:4 (**2**·DMSO) host:guest composition. The crystal structure of **1**·DMSO (2:3) is dominated by a strong bifurcated acceptor-type H bond interaction involving **1** and one of the DMSO molecules. Titration calorimetric investigations in solution also confirm the formation of a stable **1**·DMSO (1:1) complex unit, suggesting that for crystal nuclei of **1**·DMSO (2:3) the pre-formed 1:1 host–guest complex is the relevant building block while the additional molecules of DMSO fill lattice voids. In contrast, compound 2 with a *trans* configuration of the two hydroxy groups gives much weaker complexation with DMSO in solution, which is in agreement with single H-bond interaction, also realized in the crystal structure of the respective inclusion complex. Thermal decomposition (TG–DSC) measurements of the crystalline complexes supply supporting data for these findings. Copyright © 2002 John Wiley & Sons, Ltd.
Additional material for this paper is available from the epoc website at http://www.wiley.com/epoc

KEYWORDS: inclusion compounds; supramolecular interactions; crystallization; calorimetry; X-ray structure

INTRODUCTION

Non-covalent bonding interactions including ion–ion, ion–dipole, dipole–dipole, hydrogen bonding, cation–π, π–π stacking and van der Waals interactions,[1] have become a topic of increasing importance both in solution and in the solid state.[2] Self-assembly,[3] inclusion formation,[4] crystal engineering[5] and other principles of supramolecular chemistry[6] are obvious results of their working manifested in a large number of supramolecular species all being based on the presence of highly specific non-covalent bonding interactions that control their structure and packing.[7] Crystalline host–guest complexes (clathrates)[8] are one particular type of compounds among them. Although there is a certain degree of insight into the molecular packing and building principles of crystalline complexes,[9] a rational design is far from being understood.[10] Polymorphs[11] and different phases of inclusion compounds[12] obtained by recrystallization from solution are typical of these difficulties.

A previous study[13] involving compound **1** (Scheme 1) has shown that depending on the solvent system used for crystallization, i.e. toluene, toluene with a trace of chloroform, two different polymorphs of **1** or an inclusion compound with chloroform (1:1) are yielded, respectively, with the polymorph obtained from toluene and traces of chloroform and the inclusion compound with chloroform featuring very similar packing motifs. That leads one to assume that a central issue in this field should certainly refer to the role of weak supramolecular

**Correspondence to:* J. Seidel, Institut für Physikalische Chemie, TU Bergakademie Freiberg, Leipziger Strasse 29, D-09596 Freiberg/Sachsen, Germany or E. Weber, Institut für Organische Chemie, TU Bergakademie Freiberg, Leipziger Strasse 29, D-09596 Freiberg/Sachsen, Germany.
E-mail: edwin.weber@chemie.tu-freiberg.de
Contract/grant sponsor: Deutsche Forschungsgemeinschaft (DFG).
Contract/grant sponsor: Fonds der Chemischen Industrie.

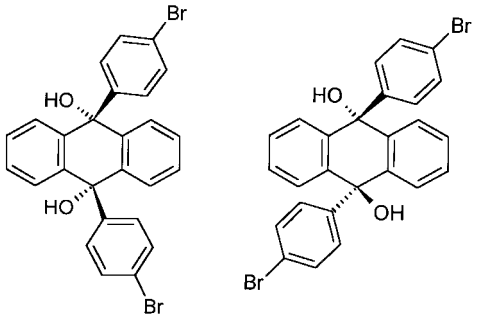

Scheme 1. Formulae of host compounds **1** and **2**

interactions existing in the precrystalline solution phase or at the very beginning of the crystallization process which may determine a subsequent crystal structure.

In this connection, particular properties proceeding from *cis* and *trans* stereoisomeric compounds **1** and **2** (Scheme 1) attracted our attention. On recrystallization from dimethyl sulfoxide (DMSO), both compounds form crystalline inclusion complexes with this solvent at which **1**·DMSO show 2:3 and **2**·DMSO 1:4 host:guest composition. The crystal structures indicated a remarkably strong hydrogen bond interaction simultaneously involving the oxygen atom of DMSO and the two hydroxyls of **1**, not being observed in **2**·DMSO. The strong interaction causes a molecular distortion of **1** and dominates also the packing structure of the inclusion crystal. These results suggested the potential use of the compound type as a model system for a study of the above problem involving possible pre-organizing non-covalent bonding interactions in solution prior to the crystallization of the inclusion compound. Therefore, isothermal titration calorimetry (ITC) was applied in order to detect and to characterize supramolecular interactions in solution quantitatively.

RESULTS AND DISCUSSION

Compounds **1**[13] and **2**[14] were synthesized in 55 and 17% yield, respectively, from 9,10-anthraquinone and 1,4-dibromobenzene using lithium or magnesium organic reactions. Both compounds contain two hydroxy groups and two *p*-bromophenyl substituents attached to the basic 9,10-dihydroanthracene subunit. However, unlike **1**, providing the two hydroxy groups and accordingly also the bromophenyls in a *cis* position, **2** shows a *trans* orientation of the respective groups. Hence the different positions of the interactive groups in **1** and **2** will have an influence on the crystalline packing, and hence will also affect their inclusion properties, as demonstrated by the inclusion compounds with DMSO. They show very different host:solvent stoichiometric ratios, i.e. 2:3 for **1** and 1:4 for **2**, the latter being exceptionally high with reference to the solvent part, which gives further encouragement to a structural study. Moreover, polymorphous structures of **1** and of a previously reported inclusion compound with chloroform[13] provide a reasonable base for comparative discussion.

Structural study

Perspective views of the molecular structures of **1** and **2**, including the numbering schemes of the atoms, are shown in Figs 1–3. Crystal data and selected experimental details are summarized in Table 1. Conformational features of the host molecules and geometric parameters of selected intermolecular interactions are listed in Tables 2 and 3.

Structure of 1·DMSO (2:3). While in unsolvated **1** (two polymorphs) and also in the inclusion compound with chloroform the 9,10-dihydroanthracene segment of the host molecule possesses a shallow boat conformation,[13] it is almost planar in the present DMSO complex (Fig. 1). This appears to be a consequence of the strong host to solvent interaction manifested in the formation of a defined H-bonded complex of **1** with DMSO where the two OH groups of **1** are involved in concurrent H bonding to the oxygen of DMSO giving rise to a bifurcated (three-center) acceptor-type hydrogen bond between **1** and DMSO (Fig. 1). Examples of crystal structures in which one molecule forms two strong H bonds to a given basic atom of a second molecule comparable to the present structural facts are rare in the literature.[15] As a result of the conformational flattening of the 9,10-dihydroanthracene subunit, the *p*-bromophenyl rings attached to the 9,10-positions of this unit also change their conformation in that rotations of about 80° around C(9)—C(15) and

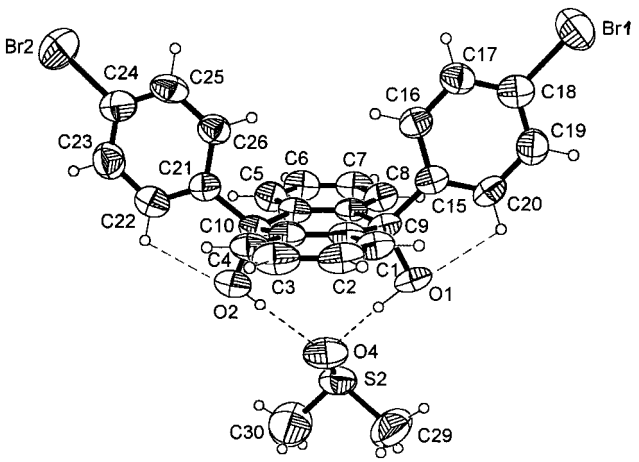

Figure 1. ORTEP plot showing the complexed host–guest unit of **1**·DMSO (2:3) with the atom labeling. Displacement ellipsoids are given at the 50% probability level. Solid and dashed lines represent covalent and non-covalent interactions, respectively

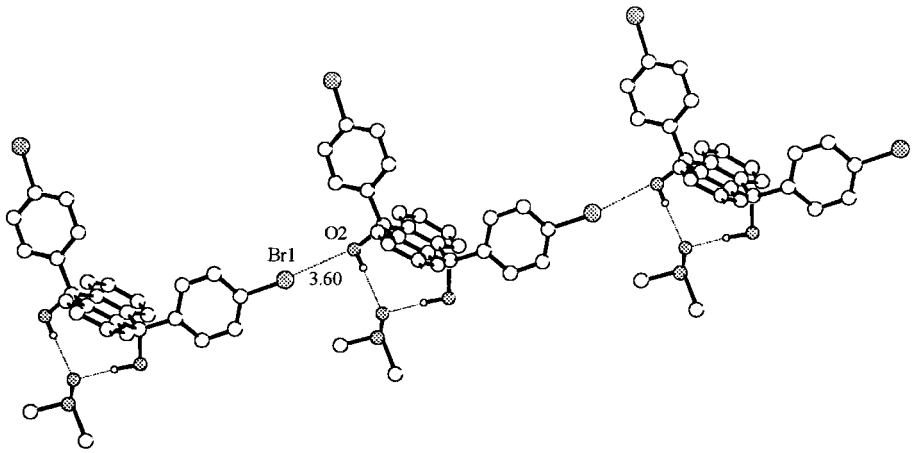

Figure 2. Packing excerpt of **1**·DMSO (2:3) illustrating the supramolecular chains of host and guest molecules arranged through H bonds and Br···O contacts, represented as dotted lines. Non-relevant H atoms are omitted for clarity

C(10)—C(21) take place in the course of which the phenyl rings change position from almost face-to-face[13] to a V-shaped geometry with the two rings nearly coplanar. In this manner, two short C—H···O-type contacts[16] involving phenyl hydrogens and hydroxy oxygens are made accessible stabilizing the whole system. It is interesting that the geometric placement resembles those formed in hypervalent (i.e. three-center, four-electron) bonds.[17]

The complex units are linked via O···Br contacts[13] to form infinite chains (Fig. 2). Packing of these chains gives rise to tubular voids that are occupied by a second DMSO species not being involved in a specific supramolecular interaction and showing statistical disorder.

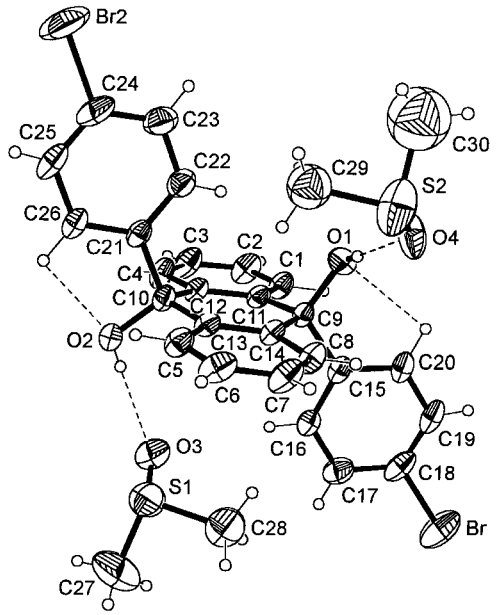

Figure 3. ORTEP plot showing the complexed host–guest unit of **2**·DMSO (1:4) with the atom labeling. Displacement ellipsoids are given at the 50% probability level. Solid and dashed lines represent covalent and non-covalent interactions, respectively

Structure of 2·DMSO (1:4). Unfortunately, a parallel between unsolvated host **2** and its inclusion compound with DMSO cannot be drawn, since the structure of unsolvated **2** is lacking. In **2**·DMSO (1:4), the host molecule does not show either a boat conformation of the central ring, such as in unsolvated **1**, or a chair conformation as in a similar compound without the bromo substituents,[18] but presents an almost planar ring conformation with the two phenyl groups being perpendicular to the central ring plane and coplanar to each other (Fig. 3). This allows the formation of short contacts between H(20)···O(1) and H(26)···O(2) (Table 2) similar to the DMSO complex of **1** (Fig. 1).

Owing to the *trans* orientation of the hydroxy groups in **2**, a pincer-type supramolecular complex corresponding to **1**·DMSO is not possible with **2**. Instead, each of the hydroxy groups of **2** form a single H bond to the oxygen atom of a DMSO molecule. By using their methyl groups, these H-bonded DMSO molecules maintain a further weak C—H···O contact to neighboring DMSO molecules not being bound to the host molecules, thus giving rise to a direct guest–guest interaction. Strands of the guest molecules are accommodated into channels formed by the host matrix which is stabilized by weak Br···Br contacts.

Thermochemical study

Results of the thermal decomposition measurements of the complexes **1**·DMSO (2:3) and **2**·DMSO (1:4) by means of simultaneous thermogravimetry–differential scanning colorimetry (TG–DSC) are shown in Fig. 4. The compound **1**·DMSO (2:3) decomposes in two steps, as expected from the structure analysis, suggesting two

Table 1. Crystal data and some selected experimental details from the crystal structures of compounds **1**·DMSO (2:3) and **2**·DMSO (1:4)

Parameter	**1**·DMSO (2:3)	**2**·DMSO (1:4)
Formula	$2(C_{26}H_{18}Br_2O_2)\cdot 3(C_2H_6OS)$	$C_{26}H_{18}Br_2O_2\cdot 4(C_2H_6OS)$
Formula mass	639.42	834.74
Temperature (K)	293(2)	200(2)
Radiation used (Å)	Cu Kα, 1.5418	Mo Kα, 0.71073
Crystal system	Monoclinic	Triclinic
Space group	*I2/a*	$P\text{-}\bar{1}$
Unit cell dimensions:		
a (Å)	20.179(1)	8.671(2)
b (Å)	13.464(1)	8.915(2)
c (Å)	22.489(1)	25.491(5)
α(°)	90	89.13(3)
β(°)	116.60(1)	89.49(3)
γ(°)	90	73.84(3)
Volume (Å^3)	5463.4(4)	1892.4(7)
Z	8	2
D_c (mg m^{-3})	1.555	1.465
Absorb. μ (mm^{-1})	5.088	2.403
F(000)	2584	856
Crystal size (mm)	0.19 × 0.36 × 0.56	0.41 × 0.38 × 0.33
Θ range for data collection (°)	3.95–64.93	2.38–30.49
Index ranges: min/max *h, k, l*	0/23, 0/15, −24/23	0/12, −11/12, −36/36
No. of reflections collected	4606	37291
Refinement method	Full-matrix/F^2	Full-matrix/F^2
Absorption correction	No correction	No correction
Data/restraints/parameters	4606/0/354	11376/0/516
Goodness-of-fit on F^2	1.057	1.042
Final *R* indices [$I > 2\sigma(I)$]	$R_1 = 0.0870$, $wR_2 = 0.232$	$R_1 = 0.0810$, $wR_2 = 0.2124$
R indices (all data)	$R_1 = 0.1120$, $wR_2 = 0.2322$	$R_1 = 0.1451$, $wR_2 = 0.2508$
Extinction coefficient	0.00025(5)	0.0019(11)
Largest diff. peak and hole (e Å^{-3})	0.92 and −0.85	0.932 and −1.191
Diffractometer	Phillips PW 1100	Enraf Nonius Kappa CCD
Data collection	$\omega - 2\Theta$ scans	ω scans

different species of included DMSO [Fig. 4(a)]. The overall mass loss in the temperature range 90–190 °C of 19.0% confirms the host:guest ratio of 2:3. The first step of guest release takes place in the temperature range 90–130 °C and is characterized by a mass loss of ∼6%, which may be assigned to the one molecule of DMSO non-bonded and statistically disordered in the crystal lattice. In the second decomposition step between 130 and 190 °C a mass loss of 13% is observed, corresponding to the guest molecules interacting with **1** through a bifurcated acceptor-type hydrogen bond. Owing to the much stronger interaction, more energy (equivalent to a higher degradation temperature) is needed for removing these particular guest molecules from the crystal lattice. Both steps of guest release are accompanied by appropriate endothermic effects in the DSC curve. In agreement with the different bonding conditions of the guest molecules in the two observed decomposition steps, the molar heats of decomposition are also very different. The release of the non-hydrogen-bonded DMSO in the temperature range 90–130 °C is accompanied by a heat effect of 48 ± 2 kJ mol^{-1} DMSO, which is of the order of magnitude of the heat of evaporation of DMSO (52.9 kJ mol^{-1}).[19] In contrast, the DMSO released at 130–160 °C is characterized by a remarkably higher heat of decomposition of 74 ± 2 kJ mol^{-1}, reflecting the strong bifurcated H bond to the host. TG and DSC effects above 240 °C can be attributed to the melting and decomposition of the pure host.

More complex are the results for the thermal degradation of **2**·DMSO (1:4) illustrated in Fig. 4(b). At least four distinguishable steps are observed in both the TG and DSC curves, not taking into account the effects above 250 °C arising from melting and decomposition of the pure host compound. The total mass loss of 37.5% in the temperature range 40–160 °C corresponds to a host:guest ratio of 1:4, which is in agreement with the x-ray structure analysis. Within this temperature range one can distinguish two main stages of mass loss. One occurs between 40 and about 120 °C and the other between 120 and 150 °C, being assigned to the two different types of host–guest interactions found in the crystal structure. However, probably owing to some overlapping of the different stages the stoichiometric ratio (two weakly interacting DMSO molecules and two hydrogen-bonded guest molecules) is not exactly reflected by steps (TG) or peaks (DSC) of equal size in the experimental curves. For the same reason, it is not possible to calculate reliable

Table 2. Selected conformational features of the host molecules **1** and **2**[a] in the DMSO complexes

Parameter	**1**	**2**
Selected torsion angles (°):		
O(1)—C(9)—C(11)—C(1)	65.7(7)	64.3(1)
O(1)—C(9)—C(14)—C(13)	111.3(7)	109.6(1)
O(1)—C(9)—C(15)—C(20)	6.5(9)	5.2(1)
C(15)—C(9)—C(11)—C(1)	−51.5(8)	−54.2(1)
C(11)—C(9)—C(15)—C(16)	−57.7(8)	−60.9(1)
C(11)—C(9)—C(15)—C(20)	124.3(7)	119.2(1)
O(2)—C(10)—C(12)—C(4)	−67.9(7)	50.3(1)
O(2)—C(10)—C(21)—C(22)	−10.7(9)	−173.0(1)
O(2)—C(10)—C(13)—C(14)	−106.4(7)	131.4(1)
C(21)—C(10)—C(12)—C(4)	49.1(8)	−65.6(1)
C atoms of the dihydroanthracene moieties are co-planar within (Å):		
Plane 1: C(1)—C(14)	−0.074 to +0.160	−0.126 to +0.073
C atoms of the bromophenyl moieties are co-planar within (Å):		
Plane 2: C(15)—C(20)	−0.012 to +0.007	−0.005 to +0.008
Plane 3: C(21)—C(26)	−0.012 to +0.017	−0.015 to +0.018
Dihedral angle between the LS planes (°):		
Planes 1–2	88.00(2)	84.32(1)
Planes 1–3	88.27(1)	88.16(1)
Planes 2–3	15.83(2)	9.45(2)

[a] Esds, where applicable, are given in parentheses.

heats of decomposition for the different stages. However, an averaged value of ca 55 ± 5 kJ mol^{-1} was estimated for the whole decomposition process. This heat effect is very close to the heat of evaporation of DMSO, demonstrating the smaller contribution of specific host–guest interactions in **2**·DMSO (1:4) compared with **1**·DMSO (2:3).

Nevertheless, on comparing the thermal degradation behavior of the two complexes **1**·DMSO (2:3) and **2**·DMSO (1:4), it is obvious that the strength of the host–guest interactions essentially determines the temperature range of the appropriate guest release. Up to about 120 °C, only weakly bonded DMSO is released. The DMSO guest molecules involved in single hydrogen bonding to one of the host hydroxyls (**2**·DMSO) are liberated between ca 120 and 150 °C, whereas the more strongly interacting DMSO molecules (via a bifurcated acceptor-type hydrogen bond to both the hydroxyls of **1**) are set free mainly above 150 °C.

Interactions in solution. As outlined above, the two compounds feature specific hydrogen bonding in their crystals, in particular **1**·DMSO (2:3), which is dominated by a bifurcated hydrogen bond involving the DMSO oxygen and the two hydroxyl groups of **1**. This raises the question of whether a corresponding interaction between the two species already exists in solution which will lead to a pre-organization of the molecules controlling the subsequent crystallization process and may ultimately determine the crystal structure. In order to prove this

Table 3. Distances and angles[a] in H bonds and short contacts of the **1**·DMSO and **2**·DMSO complexes

Atoms	Symmetry	Distance (Å) D···A	Distance (Å) D—H	Distance (Å) H···A	D—H···A angle (°)
1·DMSO (2:3):					
O(1)—H(O1)···O(4)	$-x+1, y-1/2, -z+1/2$	2.823(1)	1.07	1.76	176
O(2)—H(O2)···O(4)	$-x+1, y-1/2, -z+1/2$	2.822(1)	0.82	2.02	166
C(22)—H(22)···O(2)		2.707(1)	0.93	2.35	103
C(20)—H(20)···O(1)		2.715(1)	0.93	2.36	103
Br(1)···O(2)	$x+1/2, y+1/2, z+1/2$	3.599(1)			
2·DMSO (1:4):					
O(1)—H(1O)···O(4)	$x, y-1, z$	2.706(1)	0.79	1.92	168
O(2)—H(2O)···O(3)	$x, y-1, z$	2.704(1)	0.66	2.04	175
C(20)—H(20)···O(1)		2.798(1)	1.00	2.42	102
C(26)—H(26)···O(2)		2.682(1)	1.02	2.33	99

[a] Esds, where applicable, are given in parentheses. D, donor; A, acceptor.

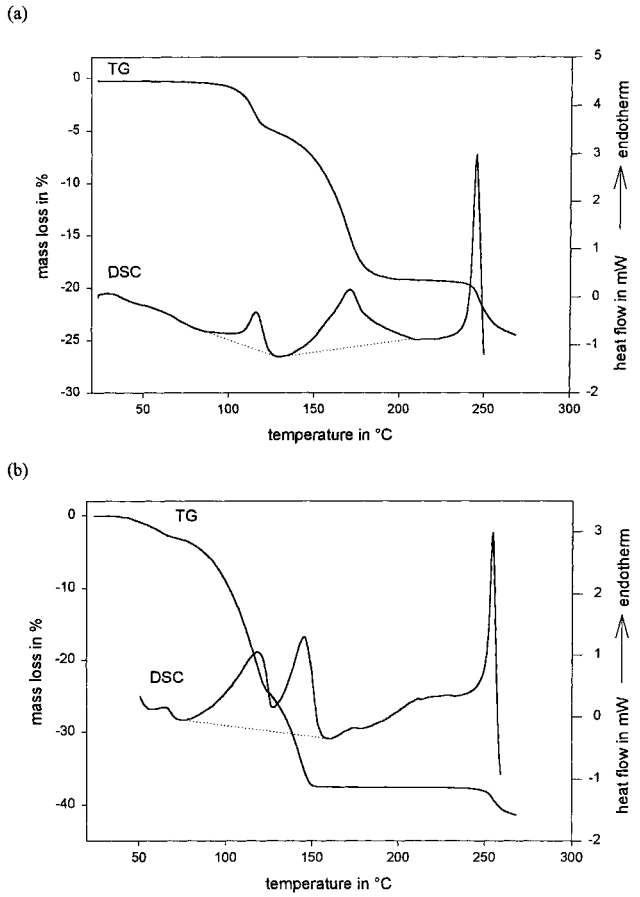

Figure 4. Thermograms (TG and DSC) for (a) **1**·DMSO (2:3) and (b) **2**·DMSO (1:4)

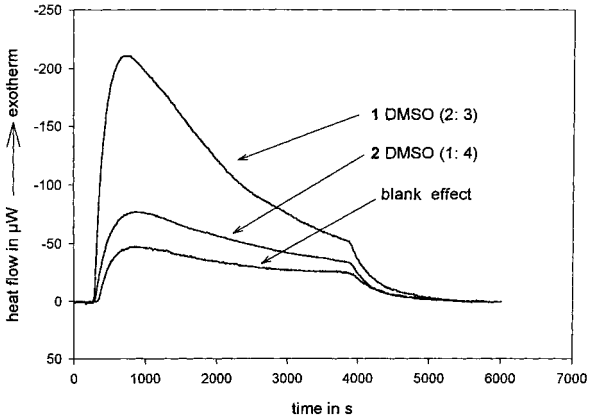

Figure 5. Results of continuous titration experiments in solution at 25 °C

hypothesis, an isothermal titration calorimetric study in solution was carried out. Considering the necessary boundary conditions,[20,21] this method is able to provide equilibrium constants, complexation enthalpies and complexation entropies. Figure 5 shows the calorimetric titration curves for the continuous runs with **1** and **2** including also the blank effect (dilution of DMSO solution into toluene).

It is obvious that the interaction between DMSO and **1** is accompanied by a remarkable larger heat effect than that for DMSO with **2**. Both calorimetric results could be fitted assuming a simple 1:1 complexation model providing the thermodynamic data summarized in Table 4. These data were confirmed by the discontinuous, incremental method in order to check for kinetic influences and no significant deviations were found.

The data involving **1** and DMSO reflect the expected stronger interaction by a relatively large exothermic enthalpy, an approximately one order of magnitude higher equilibrium constant compared with **2** with DMSO and a negative entropy of reaction. The complexation process is exclusively enthalpy driven. Therefore, it seems possible that a similar host–guest complex which dominates the crystal structure of **1**·DMSO (2:3) by a strong bifurcated acceptor-type hydrogen bond already exists in solution and controls the packing structure during crystallization, as postulated above. In contrast, the **2**·DMSO complex in solution is much less stable and the driving force $\Delta_R G$ contains a considerable part from the positive entropy change. The complexation enthalpy is only about one third of that for **1**·DMSO. This result is in agreement with simple hydrogen bond interactions suggested by the crystal structure of **2**·DMSO (1:4). Furthermore, the observed positive entropy change connected with the relatively small interaction energy and the negative entropy change (entropy penalty) related to a large exothermic interaction energy for **1**·DMSO are typical for supramolecular complexation phenomena in solution and are subject of the 'enthalpy–entropy compensation' concept.[22] In this particular case, the formation of a strong structural motif in the **1**·DMSO complex obviously overcompensates the usually positive contribution of solvation effects to the complexation entropy whereas the complexation entropy for the weaker **2**·DMSO complex is dominated by solvation effects. Consequently, the difference in the stability constants is smaller as expected from the interaction energies.

Table 4. Thermodynamic data for the complexation of **1** and **2** with DMSO at 25 °C

Host	Log K	$\Delta_R G$ (kJ mol^{-1})	$\Delta_R H$ (kJ mol^{-1})	$\Delta_R S$ (J mol^{-1} K^{-1})
1	2.45 ± 0.06	-14.0 ± 0.3	-18.6 ± 0.2	-15.4 ± 0.5
2	1.4 ± 0.2	-7.9 ± 0.8	-5.7 ± 0.2	7.3 ± 2

CONCLUSION

Complexation properties between diol host compounds **1** and **2** having defined *cis* and *trans* configurations of the hydroxy groups and DMSO as the guest that have been studied by crystal structure analysis and calorimetric estimation of interaction energies both in solution and in the crystalline state allow the following statements and conclusions.

In solution, **1** suggests formation of a stable hydrogen-bonded 1:1 complex with DMSO which is also found in the form of a pincer-type supramolecular complex stabilized by bifurcated acceptor-type hydrogen bonding in the crystalline state. Compound **2**, by structure not being able to undergo complexation similar to **1**, indicates in solution the formation of a single hydrogen-bonded complex exhibited also in the crystalline inclusion complex. Hence the crystal structures of the two inclusion complexes appear to reflect their previous history, i.e. crystallization from solution, in that the preformed complex units are used as building blocks for lattice generation, while additional molecules of DMSO act for filling interstitial space. Thermal decomposition (TG–DSC) measurements on the solid complexes are in agreement with the different binding states of guest molecules.

These results show for the compounds studied an informative model system contributing to the problem of predetermination of a crystal structure or co-crystalline material.[23] The idea is that based on the role of the host–guest interaction in the precrystalline solution phase one may classify three cases: (i) a stable host–guest complex is present in solution being a probable component of crystal formation; (ii) weak host–guest complexation exists in solution which may cause a pre-orientation of the molecules that controls the packing in the crystal, while crystallization of a specifically preformed host–guest complex is less probable; and (iii) specific host–guest interactions are absent in solution, leading to a crystal packing of individual molecules mostly steered by energetic restrictions and steric matching.

More systematic investigations in this field are required in order to confirm the conception and to obtain a deeper understanding of crystalline inclusion formation.

EXPERIMENTAL

Synthesis and sample preparation

Compounds **1**[13] and **2**[14] were prepared from 1,4-dibromobenzene and 9,10-anthraquinone with *n*-BuLi or magnesium in dry diethyl ether or diethyl ether–toluene in yields of 55 and 17%, respectively, using literature procedures. Inclusion compounds **1**·DMSO (2:3) and **2**·DMSO (1:4) were obtained by recrystallization of **1** and **2** from DMSO. The crystals which formed on cooling were collected and dried. Host:guest stoichiometric ratios were determined by ^{1}H NMR integration and TG–DSC. Crystals suitable for x-ray investigation were prepared by slow evaporation of solutions of the respective compounds in DMSO.

Crystallography

Intensity data for **1**·DMSO (2:3) and **2**·DMSO (1:4) were obtained on a Philips PW 1100 diffractometer at room temperature. The $\omega - 2\Theta$ scan mode was used. Owing to the disorder of the guest molecules, especially the sulfur atoms in structure **2**·DMSO (1:4), a low-temperature measurement at 200 K using an Enraf Nonius Kappa CCD diffractometer equipped with a CCD camera was performed. Initial structure models (SIR92[24]) were refined by full-matrix least squares on F^2 (SHELXL-97[25]) until convergence. Hydrogen atoms of —OH groups were located from difference electron density maps and the remainder of the H atoms were placed on the basis of geometric evidence. Crystal data and selected experimental details are given in Table 1.

Thermochemical analysis

The thermal degradation of the two different inclusions was studied by means of TG and DSC using a simultaneous TG–DSC 111 system (SETARAM, France). Crystals of an average size of 0.5–1 mm were taken from the mother liquor, blotted dry on filter-paper and rinsed briefly with diethyl ether in order to remove traces of DMSO on the surface of the crystals. For each measurement 3–4 mg of the sample were weighed into open standard aluminum crucibles. The temperature range for the TG–DSC runs was typically 20–280 °C at a linear heating rate of 5 K min^{-1}. Argon at a flow-rate of 20 ml h^{-1} was used as purge gas for all measurements.

Isothermal titration calorimetry (ITC)

Titration calorimetric measurements were performed at 25 °C by means of a twin heat conduction microcalorimeter of the Calvet type (DAK 1A-1, Russia). The titration insertion cell is laboratory-made and the design and properties of the titration equipment have been described in detail recently.[20] The titration calorimeter is characterized by a minimal detectable heat power of 1 μW and a long-term baseline drift <2 μW h^{-1}. The calorimetric vessel was typically filled with 2 ml of a solution of the host in toluene acting as inert solvent. Up to 2 ml of guest solution (DMSO in toluene) was added either in small increments of 0.2 ml at an injection rate of 20 ml h^{-1} (discontinuous titration) or continuously at

2 ml h^{-1}. The concentrations of host and guest solutions were ca 7 and 40 mmol l^{-1}, respectively. DMSO was used in surplus to ensure that data were collected over nearly the whole extent of reaction. Corrections for dilution effects were made by subtracting the appropriate blank effects from the calorimetric curves. Thermodynamic data (reaction enthalpy, equilibrium constant and reaction entropy) were computed by a least-squares analysis of the corrected calorimetric curves using a special computer program written on the MATLAB (MathWorks, USA) platform. The thermodynamic principle of the calculating procedure is described in detail in the literature.[20,21]

Supplementary Data

Atomic coordinates, bond lengths and angles, and thermal parameters have been deposited as supplementary data at the Cambridge Crystallographic Data Center with deposit No. CCDC 179856, 179857. Lists of the observed and calculated structure factors and the anisotropic displacement parameters for the non-hydrogen atoms may be obtained from the authors (E.W.) on request. Crystallographic data and computer graphics of the structures can also be viewed at the epoc website at http:/www.wiley.com/epoc.

Acknowledgements

E.W. and J.S. thanks the Deutsche Forschungsgemeinschaft (DFG) and the Fonds der Chemischen Industrie for financial support. This work is part of the Graduate School Programme (GRK 208) of the TU Bergakademie Freiberg supported by the DFG. T.H.B. is grateful for a scholarship from this organization and also thanks Professor F. H. Cano (CSIC, Madrid) for his cooperation. E.W. thanks Dr M. Czugler (CRC, Hungarian Academy of Sciences, Budapest) for expert advice.

REFERENCES

1. (a) Scheiner S (ed). *Molecular Interactions*. Wiley: Chichester, 1997; (b) Mascal M. *Contemp. Org. Synth.* 1994; 31–46.
2. (a) Schneider HJ, Yatsimirsky A. *Principles and Methods in Supramolecular Chemistry*. Wiley: Chichester, 2000; (b) Whitesell JK (ed). *Organized Molecular Assemblies in the Solid State*. Wiley: New York, 1999; (c) Desiraju GR. *Angew. Chem.* 1995; **107**: 2541–2548; *Angew. Chem., Int. Ed. Engl.* 1995; **34**: 2311–2327.
3. (a) Fujita M (ed). *Molecular Self-Assembly—Organic Versus Inorganic Approaches. Structure and Bonding*, vol. 96. Springer: Berlin, 2000; (b) Lindoy LF, Atkinson I. *Self-Assembly in Supramolecular Systems. Monographs in Supramolecular Chemistry*, vol. 7. Royal Society of Chemistry: Cambridge, 2000.
4. (a) Atwood JL, Davies JED, McNicol DD (eds). *Inclusion Compounds*, vols 1–3. Academic Press: London, 1984; vols 4 and 5, Oxford University Press: Oxford, 1991; (b) Weber E. In *Kirk–Othmer Encyclopedia of Chemical Technology* (4th edn), vol. **14**, Kroschwitz JI (ed). Wiley: New York, 1995; 122–154.
5. (a) Desiraju GR. *Crystal Engineering—The Design of Organic Solids. Materials Science Monographs*, vol. 54. Elsevier: Amsterdam, 1989; (b) Desiraju GR. *J. Chem. Soc., Chem. Commun.* 1997; 1475–1482; (c) Weber E (ed). *Design of Organic Solids. Topics in Current Chemistry*, vol. 198. Springer: Berlin, 1998; (d) Rogers RD, Zaworotko MJ (eds). *Crystal Engineering. ACA Transactions*, vol. 33. ACA: Ellicott Station, Buffalo, NY, 1999.
6. (a) Steed JW, Atwood JL. *Supramolecular Chemistry*. Wiley: Chichester, 2000; (b) Lehn J-M. *Supramolecular Chemistry*. VCH: Weinheim, 1995; (c) Vögtle F. *Supramolecular Chemistry*. Wiley: Chichester, 1995.
7. Atwood JL, Davies JED, McNicol DD, Vögtle F (eds). *Comprehensive Supramolecular Chemistry*, vols 1–10. Elsevier Science: Oxford, 1996.
8. (a) Weber E (ed). *Molecular Inclusion and Molecular Recognition–Clathrates I and II. Topics in Current Chemistry*, vols 140 and 149. Springer: Berlin, 1987 and 1988; (b) Bishop R. *Chem. Soc. Rev.* 1996; 311–319.
9. (a) Gavezotti A (ed). *Theoretical Aspects and Computer Modeling of the Molecular Solid State*. Wiley: Chichester, 1997; (b) Gavezotti A. *Acc. Chem. Res.* 1994; **27**: 309–314.
10. (a) Maddox J. *Nature (London)* 1988; **335**: 201; (b) Hawthorne FC. *Nature (London)* 1990; **345**: 297; (c) Wolff JJ. *Angew. Chem.* 1996; **108**: 2339–2341; *Angew. Chem., Int. Ed. Engl.* 1996; **35**: 2195–2197.
11. (a) Bernstein J. In *Organic Solid State Chemistry. Studies in Organic Chemistry*; vol. 32, Desiraju GR (ed). Elsevier: Amsterdam, 1987; 471–511; (b) Dunitz JD, Bernstein J. *Acc. Chem. Res.* 1995; **28**: 193–200; (c) Caira MR. In *Design of Organic Solids. Topics in Current Chemistry*, vol. 198, Weber E (ed). Springer: Berlin, 1998; 163–208.
12. (a) Beketov K, Weber E, Ibragimov BT, Seidel J, Köhnke K. *Adv. Mater.* 2000; **12**: 664–667; (b) Beketov K, Weber E, Seidel J, Köhnke K, Ibragimov BT. *Cryst. Eng.* 2000; **3**: 101–115.
13. Brehmer TH, Weber E, Cano FH. *J. Phys. Org. Chem.* 2000; **13**: 63–74.
14. (a) Ingold CK, Marshall PG. *J. Chem. Soc.* 1926; 3080–3089; (b) Dufraisse C, Morgoulis-Molho FJ. *Bull. Soc. Chim. Fr.* 1940; **7**: 928–930.
15. (a) Murray-Rust P, Glusker JP. *J. Am. Chem. Soc.* 1984; **106**: 1018–1025; (b) Hine J, Ahn K, Gallucci JC, Linden S. *J. Am. Chem. Soc.* 1984; **106**: 7980–7981.
16. Desiraju GR, Steiner T. *The Weak Hydrogen Bond. IUCr Monographs on Crystallography*, vol. 9. Oxford University Press: Oxford, 1999.
17. (a) Reed AE, Schleyer PR. *J. Am. Chem. Soc.* 1990; **112**: 1434–1445; (b) Musher JI. *Angew. Chem.* 1969; **81**: 68–83; *Angew. Chem., Int. Ed. Engl.* 1969; **8**: 54–68.
18. Barbour LJ, Caira MR, Nassimbeni LR. *J. Chem. Cryst.* 1994; **24**: 539–543.
19. (a) Douglas TB. *J. Am. Chem. Soc.* 1948; **70**: 2001–2002; (b) *NIST Chemistry WebBook, Standard Reference Data Program*. http://webbook.nist.gov/.
20. Kirchner R, Seidel J, Wolf G. *Thermochim. Acta*, 1998; **310**: 19–24.
21. (a) Christensen JJ, Ruckman J, Eatough DJ, Izatt RM. *Thermochim. Acta*, 1972; **3**: 203–218, 218–232 and 233–246; (b) Karlsson R., Kullberg L. *Chem. Ser.* 1976; **9**: 54–57; (c) Blandamer MJ. In *Biocalorimetry: Applications of Calorimetry in the Biological Sciences*, Ladbury JE, Chowdhry BZ (eds). Wiley: Chichester, 1998; 5–23.
22. Inoue Y, Wada T. In *Advances in Supramolecular Chemistry*, vol. 4, Gokel GW (ed). JAI Press: Greenwich, CT, 1997; 55–96.
23. Bürgi HB, Hulliger J, Langley PJ. *Curr. Opin. Solid State Mater. Sci.* 1998; **3**: 425–430.
24. Altomare A, Burla MC, Camalli M, Cascarano G, Giacovazzo C, Guagliardi A, Polidori G. *J. Appl. Crystallogr.* 1994; **27**: 435–447.
25. Sheldrick GM. SHELXL-97: Program for the Refinement of Crystal Structures. University of Göttingen: Göttingen, 1997.